

CERN-EP-2024-283

28 October 2024

Medium-induced modification of groomed and ungroomed jet mass and angularities in Pb–Pb collisions at $\sqrt{s_{\text{NN}}} = 5.02$ TeV

ALICE Collaboration*

Abstract

The ALICE Collaboration presents a new suite of jet substructure measurements in Pb–Pb and pp collisions at a center-of-mass energy per nucleon pair $\sqrt{s_{\text{NN}}} = 5.02$ TeV. These measurements provide access to the internal structure of jets via the momentum and angle of their constituents, probing how the quark–gluon plasma modifies jets, an effect known as jet quenching. Jet grooming additionally removes soft wide-angle radiation to enhance perturbative accuracy and reduce experimental uncertainties. We report the groomed and ungroomed jet mass m_{jet} and jet angularities $\lambda_{\alpha}^{\kappa}$ using $\kappa = 1$ and $\alpha > 0$. Charged-particle jets are reconstructed at midrapidity using the anti- k_{T} algorithm with resolution parameter $R = 0.2$. A narrowing of the jet mass and angularity distributions in Pb–Pb collisions with respect to pp is observed and is enhanced for groomed results, confirming modification of the jet core. By using consistent jet definitions and kinematic cuts between the mass and angularities for the first time, previous inconsistencies in the interpretation of quenching measurements are resolved, rectifying a hurdle for understanding how jet quenching arises from first principles and highlighting the importance of a well-controlled baseline. These results are compared with a variety of theoretical models of jet quenching, providing constraints on jet energy-loss mechanisms in the quark–gluon plasma.

arXiv:2411.03106v1 [nucl-ex] 5 Nov 2024

© 2024 CERN for the benefit of the ALICE Collaboration.

Reproduction of this article or parts of it is allowed as specified in the CC-BY-4.0 license.

*See Appendix A for the list of collaboration members

1 Introduction

Collisions of ultra-relativistic heavy ions at the Large Hadron Collider (LHC) allow the study of bulk properties in quantum chromodynamics (QCD) at high temperature and density. These collisions produce a strongly-interacting state of matter called the quark–gluon plasma (QGP) [1, 2] where quarks and gluons are deconfined from nucleons. The hard scattering of two partons from these collisions forms collimated sprays of particles called jets. As they traverse the QGP, the partonic jets lose energy to the medium and their internal structure is modified, an effect known as jet quenching [3–7]. Consequently, jets can probe the structure and evolution of the QGP, and provide information about QGP transport properties, degrees of freedom, and the mechanisms for energy loss, as a function of momentum scale.

Jet substructure observables, which characterize the angular and transverse momentum distributions of the particles which constitute jets, can quantify these QGP quenching effects [8, 9]. For example, the jet invariant mass, $m_{\text{jet}} \equiv \sqrt{E_{\text{jet}}^2 - p_{\text{jet}}^2}$, where E_{jet} is the jet energy and p_{jet} its total momentum, has seen extensive experimental [10–20] and theoretical [21–24] study in recent years. The generalized jet angularities [25–29] are another class of such observables, defined as

$$\lambda_{\alpha}^{\kappa} \equiv \sum_{i \in \text{jet}} \left(\frac{p_{\text{T},i}}{p_{\text{T},\text{jet}}} \right)^{\kappa} \left(\frac{\Delta R_i}{R} \right)^{\alpha}, \quad (1)$$

where i runs over constituents in the jet, p_{T} designates transverse momentum, R is the jet resolution parameter, and $\Delta R_i \equiv \sqrt{(y_{\text{jet}} - y_i)^2 + (\varphi_{\text{jet}} - \varphi_i)^2}$ gives the distance between the jet axis and its i th constituent in the rapidity (y) – azimuthal angle (φ) plane. The continuous parameters α and κ define the specific observable, where the $\kappa = 1$ and $\alpha > 0$ configurations are infrared and collinear (IRC) safe [30].

Both m_{jet} and $\lambda_{\alpha}^{\kappa}$ characterize the jet radial energy profile, with a direct theoretical relation between them,

$$\lambda_2^1 = \left(\frac{m_{\text{jet}}}{p_{\text{T},\text{jet}} R} \right)^2 + \mathcal{O}[(\lambda_2^1)^2], \quad (2)$$

where λ_2^1 is also called the jet thrust [31], and the last term contains higher-order corrections in m_{jet} [32]. The jet thrust is also related to the jet girth [33], $g = \lambda_1^1 R$, with a smaller angular weighting α . The ALICE collaboration measured g and m_{jet} in Pb–Pb collisions during LHC Run 1 at nucleon–nucleon center-of-mass energy $\sqrt{s_{\text{NN}}} = 2.76$ TeV, and compared the results to Monte Carlo models of pp collisions [11, 34]. Significant quenching modification was observed for g , while no significant modification was seen for m_{jet} . Since g and m_{jet} are theoretically related, this discrepancy was unexpected. These measurements differed in their ranges of $p_{\text{T},\text{jet}}$, associated with quenching strength and nonperturbative dependence, as well as the angular weighting α , associated with momentum broadening, which both could account for the discrepancy.

This letter presents angularities for the 10% most central Pb–Pb collisions at $\sqrt{s_{\text{NN}}} = 5.02$ TeV. A recent measurement of IRC-safe angularities in pp collisions at identical center-of-mass energy is used as a no-quenching baseline [35]. We preserve the notation $\lambda_{\alpha} \equiv \lambda_{\alpha}^1$ from this measurement, and compare these angularities with new measurements of m_{jet} using the same pp and Pb–Pb collision data, using equivalent R for the first time to address the girth–mass inconsistency. The results are reported for background-subtracted charged-particle jets with transverse momenta of $40 < p_{\text{T}}^{\text{ch,jet}} < 60$ GeV/ c .

Soft drop grooming [36] is employed to remove soft wide-angle radiation from jets, minimizing the nonperturbative dependence of m_{jet} and λ_{α} . Systematically varying $p_{\text{T},\text{jet}}$, α , R , and grooming for each observable provides coherent constraints on models of jet quenching.

2 Experimental setup and datasets

A description of the ALICE detector and its performance is given in Refs. [37, 38]. The pp data were collected in 2017 at $\sqrt{s} = 5.02$ TeV during Run 2 of the CERN LHC [39] using a minimum-bias trigger, which requires a coincidence of hits in two forward V0 scintillator detectors [40]. The Pb–Pb data were collected during 2018 at $\sqrt{s_{NN}} = 5.02$ TeV, using high-multiplicity events in the V0 detectors to trigger on the 10% most central collisions (0–10% centrality class) [41]. The event selection includes a primary-vertex selection and the removal of beam-induced background events and pileup [42]. The pp data sample contains 870 million events and corresponds to an integrated luminosity of 18.0 ± 0.4 nb⁻¹ [43]. The 0-10% centrality Pb–Pb data sample contains 91.2 million events, corresponding to an integrated luminosity of 0.119 ± 0.003 nb⁻¹ [44].

Charged-particle tracks are reconstructed using information from both the Time Projection Chamber (TPC) [45] and the Inner Tracking System (ITS) [46], using both global tracks and complementary tracks. Global tracks are required to include at least one hit in the silicon pixel detector (SPD), comprising the two innermost layers of the ITS, and to satisfy a number of quality criteria [47]. Complementary tracks do not contain any hits in the SPD, but otherwise satisfy the tracking criteria, and are refit using the primary vertex of the event to constrain their trajectory. Including complementary tracks ensures approximately uniform azimuthal acceptance, while preserving similar p_T resolution to tracks with SPD hits. Tracks with $0.15 < p_T < 100$ GeV/ c are accepted over the pseudorapidity range $|\eta| < 0.9$. The accepted tracks exhibit a momentum resolution ranging from about 1% at track $p_T = 1$ GeV/ c to 4% at track $p_T = 50$ GeV/ c .

3 Analysis method

Jets are reconstructed from charged-particle tracks with FastJet 3.3.3 [48] using the anti- k_T algorithm [49] with E -scheme recombination and resolution parameter $R = 0.2$. This small value of R reduces contamination from combinatorial jets at low $p_T^{\text{ch,jet}}$ in Pb–Pb data, thereby increasing overlap with the measured vacuum baseline [35]. Despite track-based observables being collinear-unsafe [50], they offer greater momentum and angular precision than calorimeter-based observables. The π^\pm -meson mass is assumed for all jet constituents, and the jet pseudorapidity η_{jet} is required to be within the fiducial volume of the TPC, $|\eta_{\text{jet}}| < 0.9 - R$. For pp collisions, all reconstructed jets in the range $5 < p_T^{\text{ch,jet}} < 200$ GeV/ c are analyzed. In heavy-ion collisions, jets are influenced by a large background from the underlying event (UE) [51], owing to the large number of soft, thermally-produced particles from the QGP. To reduce this thermal background, the event-by-event constituent subtraction method is used [52], which adds “ghosts” to the event over the entire acceptance. These ghosts, whose small transverse momentum is calculated from the average background density, are then combined with real local particles within a maximum recombination distance $R_{\text{max}} = 0.1$. When combined, the softer (lower p_T) particle of the pair is removed from the event, while its p_T and mass is subtracted from that of the harder particle. After background subtraction, the measured range is truncated to $40 < p_T^{\text{ch,jet}} < 200$ GeV/ c before applying corrections.

Jets are groomed using soft drop [36], which reclusters the jet into an angularly-ordered tree using the Cambridge/Aachen algorithm [53] before iterating along the hardest branch and trimming away soft, wide-angle radiation at each splitting until the soft drop condition is satisfied, $p_{T,\text{min}}/(p_{T,\text{min}} + p_{T,\text{max}}) > z_{\text{cut}}(\Delta R/R)^\beta$, where $p_{T,i}$ are the transverse momenta of the branches and z_{cut} and β are user parameters, which are set to 0.2 and 0, respectively. These settings require the jet to have a splitting where the softer branch carries 20% or more of the total transverse momentum of the splitting (i.e., $z_{\text{cut}} = 0.2$) independent of the angle of the splitting (i.e., $\beta = 0$), which improves the efficiency of tagging the first hard splitting in the large background of Pb–Pb collisions [54].

The reconstructed jet mass and jet angularity distributions are affected by tracking inefficiency, particle interactions with detector material, and finite track p_T resolution. Moreover, the background subtraction

procedure in Pb–Pb collisions only corrects for the average UE, and remaining background fluctuations smear the reconstructed distributions. To account for these effects, pp events are simulated with the PYTHIA 8 generator using the Monash 2013 tune [55] and passed through a setup of the ALICE detector using GEANT3 [56] to account for the particle transport through the detector material. For the Pb–Pb analysis, the PYTHIA 8 simulations including GEANT3 reconstruction (detector level) are embedded into reconstructed Pb–Pb data events (combined level). Background subtraction and jet reconstruction are performed on the combined-level events, identical to the data analysis. Jets are matched geometrically between the detector (in pp) or combined (in Pb–Pb) level to the jets reconstructed from the PYTHIA 8 simulation without detector effects (truth-level), with these jet matches required to be unique. In Pb–Pb, the matched combined-level jet must contain tracks from the detector-level jet amounting to at least 50% of the p_T of the detector-level jet. These requirements allow for a reliable estimation of background effects and fluctuations on the observables.

A four-dimensional response matrix (RM) describing the detector and background response in $p_T^{\text{ch jet}}$ and λ_α or m_{jet} is constructed from the jets matched between detector-level (combined-level) and generator-level and used in a two-dimensional unfolding with the iterative Bayesian unfolding algorithm [57] as implemented in RooUnfold [58]. The number of iterations through the unfolding was optimized by ensuring good closure of the unfolding procedure at the earliest iteration, with values ranging from 5 to 15 depending on the collision system and $p_T^{\text{ch jet}}$ interval. More details on the background subtraction and jet matching can be found in Ref. [59].

4 Systematic uncertainties

The systematic uncertainties for the observables reported in this paper are estimated from the uncertainty on the tracking efficiency, the unfolding, and the dependence on the event generator used in the simulations. In Pb–Pb, additional uncertainties arise from the estimation of the thermal background and the background subtraction procedure. Variations to the analysis procedure (described below) are performed to estimate these uncertainties, with the relative variation between unfolded distributions obtained with the default and modified procedures taken as the relative systematic uncertainty. The total systematic uncertainty is then taken as the quadratic sum of all contributions. The procedure is the same with and without grooming.

The systematic uncertainty due to the tracking efficiency uncertainty is evaluated using random rejection of tracks before jet finding. The tracking efficiency uncertainty is estimated to be 3% in pp and 3–5% in Pb–Pb collisions, depending on track p_T , based on variations in the track selection criteria and on the ITS–TPC track-matching efficiency uncertainty. The RM is recreated after randomly rejecting the fraction of tracks equal to the corresponding uncertainty, and the results are unfolded. The systematic uncertainty arising from the unfolding regularization is evaluated by varying the number of unfolding iterations by ± 2 units, altering the shape of the prior distribution, changing the detector-level observable binning, and truncating the lower and upper bounds in the detector-level charged-particle jet transverse momentum $p_{T,\text{det}}^{\text{ch jet}}$ range by 5 and 80 GeV/ c , respectively. The systematic uncertainty due to the model dependence of the generator used to construct the response matrix is estimated by comparing results obtained via unfolding with RMs generated using PYTHIA 8 [55] and HERWIG 7 [60, 61] for the pp and Pb–Pb analyses, and also JEWEL [62] for the Pb–Pb analysis. The systematic uncertainty introduced by the background subtraction in Pb–Pb collisions using the constituent subtraction procedure is estimated by varying R_{max} from “under-subtraction” ($R_{\text{max}} = 0.05$) to “over-subtraction” ($R_{\text{max}} = 0.5$), around the nominal value of $R_{\text{max}} = 0.1$. The uncertainty due to residual contamination from the uncorrelated thermal background produced by the QGP is estimated by embedding combined-level MC jets into a simulated thermal background and applying the analysis procedure, with any non-closure observed in the unfolding taken as a systematic uncertainty. The total relative systematic uncertainty ranges from 2% to 26% for λ_α and 3% to 30% for m_{jet} , with larger values in the tails of the λ_α and m_{jet} distributions and lower $p_T^{\text{ch jet}}$

intervals. See Ref. [59] for more details about the systematic uncertainties used in this measurement.

5 Results

In this letter we report the m_{jet} and λ_α distributions in the charged-jet transverse momentum interval $40 < p_{\text{T}}^{\text{ch jet}} < 60$ GeV/ c in inclusive pp and central (0–10%) Pb–Pb collisions; additional $p_{\text{T}}^{\text{ch jet}}$ ranges from 60 to 150 GeV/ c are reported in Ref. [59]. The inclusive jet angularities from Ref. [35], measured in pp collisions at $\sqrt{s} = 5.02$ TeV, are used as a baseline for these Pb–Pb results. The distributions are reported both with and without soft drop grooming (using the parameters $z_{\text{cut}} = 0.2$ and $\beta = 0$) as normalized differential cross sections,

$$\frac{1}{\sigma} \frac{d\sigma}{d\lambda_\alpha} \equiv \frac{1}{N_{\text{jets}}} \frac{dN_{\text{jets}}}{d\lambda_\alpha} \text{ (ungroomed), \quad or \quad } \frac{1}{\sigma_{\text{inc}}} \frac{d\sigma}{d\lambda_{\alpha,\text{g}}} \equiv \frac{1}{N_{\text{jets}}} \frac{dN_{\text{gr jets}}}{d\lambda_{\alpha,\text{g}}} \text{ (groomed),} \quad (3)$$

where N_{jets} is the number of inclusive (ungroomed) jets within a given $p_{\text{T}}^{\text{ch jet}}$ range and σ is the corresponding cross section. For the groomed case, some jets (including all single-particle jets) are removed by the grooming procedure, and therefore the cross section is explicitly normalized by the number of inclusive (ungroomed) jets; for the ungroomed case, $\sigma = \sigma_{\text{inc}}$. The analog of Eq. 3 also applies for m_{jet} .

Figure 1 shows the ungroomed m_{jet} and groomed $m_{\text{jet,g}}$ distributions for $40 < p_{\text{T}}^{\text{ch jet}} < 60$ GeV/ c , while the ungroomed λ_α distributions are shown in Fig. 2 and the groomed λ_α distributions are displayed in Fig. 3. The distributions from Pb–Pb collisions are compared to pp data and several models, with Pb–Pb/pp ratios displayed in the bottom panels. The relative uncertainties are assumed to be uncorrelated between collision systems, and theoretical error bands are purely statistical. The ratios suggest an enhancement at small values of angularity and mass and a corresponding suppression at large values, consistent with jet “narrowing,” i.e. the transverse momentum becoming more collimated along the jet axis; systematic uncertainties, however, are significant, especially for ungroomed m_{jet} .

Quenching modification of the ungroomed jet girth (λ_1), as quantified in the Pb–Pb/pp ratio, is smaller than when using a MC simulated pp baseline generated with PYTHIA 8, where both tails of the ratio are modified by an approximate factor of 2 [34]. This difference is explained by an approximate 20% difference between the central values of the pp data and PYTHIA 8 simulation in the tails of the distribution [59]. This difference, which enhanced the observed quenching effects in Ref. [34], highlights the importance of measuring a proper vacuum baseline for jet quenching. Modification of the jet thrust λ_2 is more significant than m_{jet} , despite the theoretical relation given in Eq. 2.

Comparisons to various theoretical calculations are shown. JETSCAPE [63] uses a medium-modified parton shower described by MATTER [64] for the high-virtuality phase and Linear Boltzmann Transport (LBT) [65] for the low-virtuality phase. Higher-Twist parton energy loss calculations [66] use POWHEG [67] + PYTHIA 6 as a vacuum baseline; as the partons traverse the QGP, they probabilistically emit medium-induced gluon radiation following the \hat{q} -dependent Higher-Twist formalism [68–71]. Finally, the Hybrid model [72] allows partons produced by a vacuum shower to undergo medium interactions according to a strongly-coupled AdS/CFT-based model. Two variations are given, where partons do or do not interact via in-medium elastic Molière scattering [73], which scatters particles at large angles and broadens both m_{jet} and λ_α . Individual comparisons of groomed and ungroomed m_{jet} and λ_α distributions between pp and Pb–Pb data and model predictions are reported in Ref. [59].

Models show general agreement with the measured Pb–Pb/pp ratios within uncertainties. However, data disfavors the Hybrid model with in-medium elastic scattering at large m_{jet} (2.3σ difference in the last bin) but slightly favors it at large λ_α ($\alpha = 2$ exhibits a 0.94σ difference in the last bin, as compared to 1.8σ for no elastic scattering). While Eq. 2 relates m_{jet} and λ_2 directly to one another, model comparisons show differing behavior within this kinematic regime. Since the distributions are positive definite and obey square proportionality following Eq. 2, large corrections to this equation must apply at these

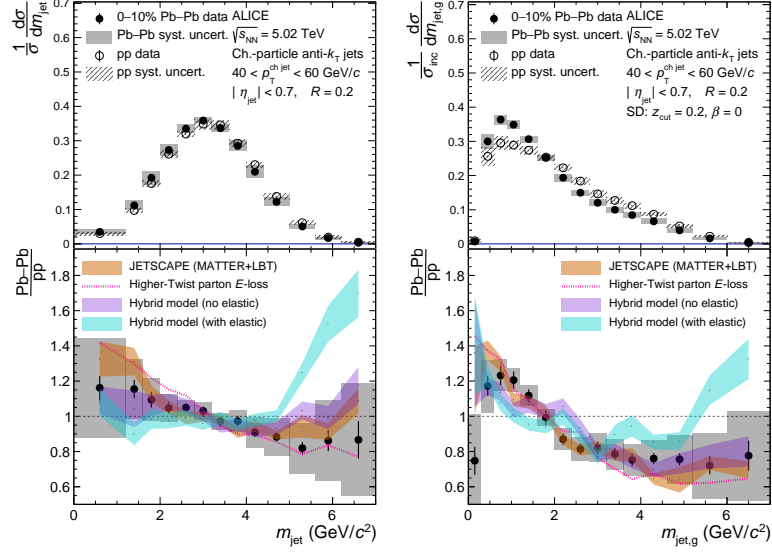


Figure 1: ALICE measurements of ungroomed m_{jet} (left) and groomed $m_{\text{jet,g}}$ (right) using $R = 0.2$ charged-particle jets with $40 < p_{\text{T}}^{\text{ch,jet}} < 60$ GeV/c in pp and Pb–Pb collisions at $\sqrt{s_{\text{NN}}} = 5.02$ TeV compared to models. The bottom panel shows the ratio of Pb–Pb distributions to pp, which quantifies the substructure modifications from quenching.

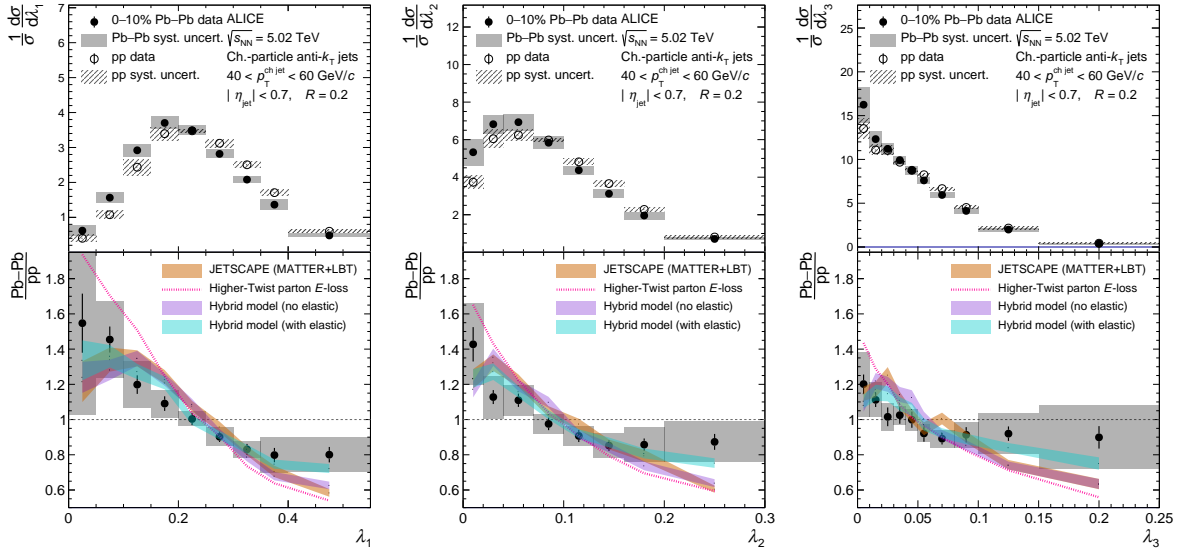


Figure 2: ALICE measurements of ungroomed λ_{α} for $\alpha = 1$ ('girth,' left), $\alpha = 2$ ('thrust,' center), and $\alpha = 3$ (right) using $R = 0.2$ charged-particle jets with $40 < p_{\text{T}}^{\text{ch,jet}} < 60$ GeV/c in pp and Pb–Pb collisions at $\sqrt{s_{\text{NN}}} = 5.02$ TeV compared to models. The bottom panel shows the ratio of Pb–Pb distributions to pp, which quantifies the substructure modifications from quenching.

values of $p_{\text{T}}^{\text{ch,jet}}$. These could include nonperturbative effects such as hadronization as well as higher-order correction terms $\mathcal{O}[(\lambda_2)^2]$, which both could be significant at these smaller values of $p_{\text{T}}^{\text{ch,jet}}$ where the strong coupling α_s is large. Therefore, despite the close mathematical relationship, the observables remain different. Underlying physical differences also exist, as jet mass is sensitive to quark masses, whereas the IRC-safe jet angularities are more sensitive to the angular profile of jet fragmentation. The behavioral discrepancies between the measured distributions originate from these physical differences of the observables themselves, which clarifies the girth–mass discrepancy observed between earlier measurements. This observation highlights the importance of making broad measurements of quenched

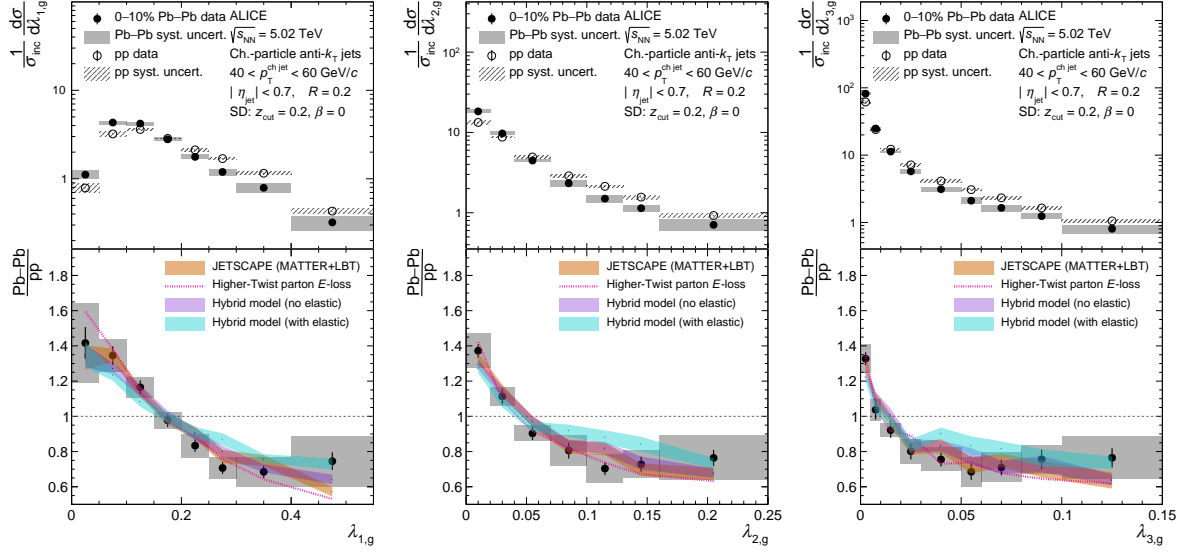


Figure 3: ALICE measurements of groomed $\lambda_{\alpha,g}$ for $\alpha = 1$ (‘girth,’ left), $\alpha = 2$ (‘thrust,’ center), and $\alpha = 3$ (right) using $R = 0.2$ charged-particle jets with $40 < p_T^{\text{ch,jet}} < 60$ GeV/c in pp and Pb–Pb collisions at $\sqrt{s_{\text{NN}}} = 5.02$ TeV compared to models. The bottom panel shows the ratio of Pb–Pb distributions to pp, which quantifies the substructure modifications from quenching. These ratios are visibly enhanced as compared to the ungroomed distributions shown in Fig. 2, signifying a strongly quenched jet core.

jet substructure, as closely-related observables can provide significantly different probes of underlying physical phenomena.

Increasing the value of α in Fig. 2 correspondingly increases the weight of wide-angle jet constituents, which are more affected by nonperturbative processes [32, 35]. Less narrowing is observed with increased α for the ungroomed λ_α , revealing a strongly quenched jet core. This conclusion is supported by a significant enhancement in the narrowing effect of λ_α for jets groomed with soft drop, comparing Figs. 2 and 3. Removing soft, wide angle jet constituents substantially modifies the shapes of the groomed distributions, with the distributions of $m_{\text{jet},g}$ and $\lambda_{\alpha,g}$ peaking at lower values than m_{jet} and λ_α . Soft drop grooming also reduces systematic uncertainties via limiting the effects from tracking inefficiency and generator dependence. Nevertheless, most models describe the groomed observables better than the ungroomed ones, despite the smaller uncertainties of the groomed results, as grooming reduces the influence of soft, wide-angle radiation thus improving theoretical control.

6 Conclusions

In this letter, measurements of jet mass and angularities in pp and Pb–Pb collisions at $\sqrt{s_{\text{NN}}} = 5.02$ TeV are presented. The medium-induced jet modifications in Pb–Pb collisions are explored both with and without grooming. These results depict a consistent picture of narrowing as jets traverse the QGP, which is dominated by a collinearized jet core. By measuring both m_{jet} and jet thrust (λ_2) using the same jets, and by also measuring the appropriate pp baseline, we reexamine the inconsistency between the girth and mass distributions raised by earlier measurements, which showed conflicting quenching behavior in these related observables. Fundamental differences are found between these observables at low $p_T^{\text{ch,jet}}$ ($40 < p_T^{\text{ch,jet}} < 60$ GeV/c) also in the analysis presented in this letter. This indicates that the mass–thrust relation (Eq. 2) must depend on significant higher-order corrections or on nonperturbative physics at low $p_T^{\text{ch,jet}}$, where the strong coupling α_S is large.

The data generally agree with models including in-medium energy loss. The jet mass prefers no in-medium elastic Molière scattering (within the Hybrid model), but the jet angularities slightly prefer if

this process is included. Future studies are needed to understand these model discrepancies. Theory comparisons also reveal that a pp baseline is essential for evaluating quenching behavior of jet substructure and should always be measured to fully profit from heavy-ion runs at the LHC. Compared to previous measurements using a MC simulated pp baseline, the quenching effects are smaller.

While jet grooming has been used in many recent measurements, the phase space of groomed observables remains mostly unexplored. Using grooming to reduce experimental uncertainties while selecting observables which probe effects such as in-medium color coherence will be essential to illuminate medium structure and the origins of jet quenching. Grooming can also be used to reduce nonperturbative effects, providing a handle to isolate these mechanisms in the QGP.

Acknowledgements

We gratefully acknowledge Daniel Pablos Alfonso, Krishna Rajagopal, Yasuki Tachibana, Abhijit Majumder, Shi-Yong Chen (陈时勇), and Ben-Wei Zhang (张本威) for providing theoretical predictions for these results and for engaging in many useful discussions.

The ALICE Collaboration would like to thank all its engineers and technicians for their invaluable contributions to the construction of the experiment and the CERN accelerator teams for the outstanding performance of the LHC complex. The ALICE Collaboration gratefully acknowledges the resources and support provided by all Grid centres and the Worldwide LHC Computing Grid (WLCG) collaboration. The ALICE Collaboration acknowledges the following funding agencies for their support in building and running the ALICE detector: A. I. Alikhanyan National Science Laboratory (Yerevan Physics Institute) Foundation (ANSL), State Committee of Science and World Federation of Scientists (WFS), Armenia; Austrian Academy of Sciences, Austrian Science Fund (FWF): [M 2467-N36] and Nationalstiftung für Forschung, Technologie und Entwicklung, Austria; Ministry of Communications and High Technologies, National Nuclear Research Center, Azerbaijan; Conselho Nacional de Desenvolvimento Científico e Tecnológico (CNPq), Financiadora de Estudos e Projetos (Finep), Fundação de Amparo à Pesquisa do Estado de São Paulo (FAPESP) and Universidade Federal do Rio Grande do Sul (UFRGS), Brazil; Bulgarian Ministry of Education and Science, within the National Roadmap for Research Infrastructures 2020-2027 (object CERN), Bulgaria; Ministry of Education of China (MOEC), Ministry of Science & Technology of China (MSTC) and National Natural Science Foundation of China (NSFC), China; Ministry of Science and Education and Croatian Science Foundation, Croatia; Centro de Aplicaciones Tecnológicas y Desarrollo Nuclear (CEADEN), Cubaenergía, Cuba; Ministry of Education, Youth and Sports of the Czech Republic, Czech Republic; The Danish Council for Independent Research | Natural Sciences, the VILLUM FONDEN and Danish National Research Foundation (DNRF), Denmark; Helsinki Institute of Physics (HIP), Finland; Commissariat à l’Energie Atomique (CEA) and Institut National de Physique Nucléaire et de Physique des Particules (IN2P3) and Centre National de la Recherche Scientifique (CNRS), France; Bundesministerium für Bildung und Forschung (BMBF) and GSI Helmholtzzentrum für Schwerionenforschung GmbH, Germany; General Secretariat for Research and Technology, Ministry of Education, Research and Religions, Greece; National Research, Development and Innovation Office, Hungary; Department of Atomic Energy Government of India (DAE), Department of Science and Technology, Government of India (DST), University Grants Commission, Government of India (UGC) and Council of Scientific and Industrial Research (CSIR), India; National Research and Innovation Agency - BRIN, Indonesia; Istituto Nazionale di Fisica Nucleare (INFN), Italy; Japanese Ministry of Education, Culture, Sports, Science and Technology (MEXT) and Japan Society for the Promotion of Science (JSPS) KAKENHI, Japan; Consejo Nacional de Ciencia (CONACYT) y Tecnología, through Fondo de Cooperación Internacional en Ciencia y Tecnología (FONCICYT) and Dirección General de Asuntos del Personal Académico (DGAPA), Mexico; Nederlandse Organisatie voor Wetenschappelijk Onderzoek (NWO), Netherlands; The Research Council of Norway, Norway; Pontificia Universidad Católica del Perú, Peru; Ministry of Science and Higher Education, National Science

Centre and WUT ID-UB, Poland; Korea Institute of Science and Technology Information and National Research Foundation of Korea (NRF), Republic of Korea; Ministry of Education and Scientific Research, Institute of Atomic Physics, Ministry of Research and Innovation and Institute of Atomic Physics and Universitatea Nationala de Stiinta si Tehnologie Politehnica Bucuresti, Romania; Ministry of Education, Science, Research and Sport of the Slovak Republic, Slovakia; National Research Foundation of South Africa, South Africa; Swedish Research Council (VR) and Knut & Alice Wallenberg Foundation (KAW), Sweden; European Organization for Nuclear Research, Switzerland; Suranaree University of Technology (SUT), National Science and Technology Development Agency (NSTDA) and National Science, Research and Innovation Fund (NSRF via PMU-B B05F650021), Thailand; Turkish Energy, Nuclear and Mineral Research Agency (TENMAK), Turkey; National Academy of Sciences of Ukraine, Ukraine; Science and Technology Facilities Council (STFC), United Kingdom; National Science Foundation of the United States of America (NSF) and United States Department of Energy, Office of Nuclear Physics (DOE NP), United States of America. In addition, individual groups or members have received support from: Czech Science Foundation (grant no. 23-07499S), Czech Republic; FORTE project, reg. no. CZ.02.01.01/00/22_008/0004632, Czech Republic, co-funded by the European Union, Czech Republic; European Research Council (grant no. 950692), European Union; ICSC - Centro Nazionale di Ricerca in High Performance Computing, Big Data and Quantum Computing, European Union - NextGenerationEU; Academy of Finland (Center of Excellence in Quark Matter) (grant nos. 346327, 346328), Finland; Deutsche Forschungs Gemeinschaft (DFG, German Research Foundation) “Neutrinos and Dark Matter in Astro- and Particle Physics” (grant no. SFB 1258), Germany.

References

- [1] J. D. Bjorken, “Highly relativistic nucleus-nucleus collisions: The central rapidity region”, *Phys. Rev. D* **27** (1983) 140–151.
- [2] W. Busza, K. Rajagopal, and W. van der Schee, “Heavy ion collisions: The big picture and the big questions”, *Annu. Rev. Nucl. Part. Sci.* **68** (2018) 339–376, arXiv:1802.04801 [hep-ph].
- [3] J. D. Bjorken, “Energy Loss of Energetic Partons in Quark-Gluon Plasma: Possible Extinction of High p_T jets in Hadron-Hadron Collisions.” Fermilab, 1982.
<https://lss.fnal.gov/archive/preprint/fermilab-pub-82-059-t.shtml>.
- [4] D. A. Appel, “Jets as a probe of quark-gluon plasmas”, *Phys. Rev. D* **33** (1986) 717–722.
- [5] M. Gyulassy and M. Plümer, “Jet Quenching in Dense Matter”, *Phys. Lett. B* **243** (1990) 432–438.
- [6] R. Baier, Y. Dokshitzer, S. Peigné, and D. Schiff, “Induced gluon radiation in a QCD medium”, *Phys. Lett. B* **345** (1995) 277–286, arXiv:hep-ph/9411409.
- [7] S. Cao and X.-N. Wang, “Jet quenching and medium response in high-energy heavy-ion collisions: a review”, *Rep. Prog. Phys.* **84** (2021) 024301.
- [8] Y. Mehtar-Tani and K. Tywoniuk, “Groomed jets in heavy-ion collisions: sensitivity to medium-induced bremsstrahlung”, *JHEP* **4** (2017) 125, arXiv:1610.08930 [hep-ph].
- [9] Y.-T. Chien and R. Kunnawalkam Elayavalli, “Probing heavy ion collisions using quark and gluon jet substructure”, arXiv:1803.03589 [hep-ph].
- [10] CMS Collaboration, S. Chatrchyan *et al.*, “Studies of jet mass in dijet and W/Z + jet events”, *JHEP* **5** (2013) 090, arXiv:1303.4811 [hep-ex].
- [11] ALICE Collaboration, S. Acharya *et al.*, “First measurement of jet mass in Pb–Pb and p–Pb collisions at the LHC”, *Phys. Lett. B* **776** (2018) 249–264, arXiv:1702.00804 [nucl-ex].

- [12] **CMS** Collaboration, A. M. Sirunyan *et al.*, “Measurement of the jet mass in highly boosted $t\bar{t}$ events from pp collisions at $\sqrt{s} = 8$ TeV”, *Eur. Phys. J. C* **77** (2017) 467, arXiv:1703.06330 [hep-ex].
- [13] **ATLAS** Collaboration, M. Aaboud *et al.*, “A measurement of the soft-drop jet mass in pp collisions at $\sqrt{s} = 13$ TeV with the ATLAS detector”, *Phys. Rev. Lett.* **121** (2018) 092001, arXiv:1711.08341 [hep-ex].
- [14] **CMS** Collaboration, A. M. Sirunyan *et al.*, “Measurement of the groomed jet mass in PbPb and pp collisions at $\sqrt{s_{NN}} = 5.02$ TeV”, *JHEP* **10** (2018) 161, arXiv:1805.05145 [hep-ex].
- [15] **CMS** Collaboration, A. M. Sirunyan *et al.*, “Measurements of the differential jet cross section as a function of the jet mass in dijet events from proton-proton collisions at $\sqrt{s} = 13$ TeV”, *JHEP* **11** (2018) 113, arXiv:1807.05974 [hep-ex].
- [16] **ATLAS** Collaboration, M. Aaboud *et al.*, “Properties of $g \rightarrow b\bar{b}$ at small opening angles in pp collisions with the ATLAS detector at $\sqrt{s} = 13$ TeV”, *Phys. Rev. D* **99** (2019) 052004, arXiv:1812.09283 [hep-ex].
- [17] **ATLAS** Collaboration, G. Aad *et al.*, “A measurement of soft-drop jet observables in pp collisions with the ATLAS detector at $\sqrt{s} = 13$ TeV”, *Phys. Rev. D* **101** (2020) 052007, arXiv:1912.09837 [hep-ex].
- [18] **ATLAS** Collaboration, G. Aad *et al.*, “Measurement of the jet mass in high transverse momentum $Z(\rightarrow b\bar{b})\gamma$ production at $\sqrt{s} = 13$ TeV using the ATLAS detector”, *Phys. Lett. B* **812** (2021) 135991, arXiv:1907.07093 [hep-ex].
- [19] **CMS** Collaboration, A. M. Sirunyan *et al.*, “Measurement of the jet mass distribution and top quark mass in hadronic decays of boosted top quarks in pp collisions at $\sqrt{s} = 13$ TeV”, *Phys. Rev. Lett.* **124** (2020) 202001, arXiv:1911.03800 [hep-ex].
- [20] **CMS** Collaboration, A. Tumasyan *et al.*, “Measurement of the differential $t\bar{t}$ production cross section as a function of the jet mass and extraction of the top quark mass in hadronic decays of boosted top quarks”, *Eur. Phys. J. C* **83** (2023) 560, arXiv:2211.01456 [hep-ex].
- [21] M. Dasgupta, A. Fregoso, S. Marzani, and G. P. Salam, “Towards an understanding of jet substructure”, *JHEP* **09** (2013) 029, arXiv:1307.0007 [hep-ph].
- [22] S. Marzani, L. Schunk, and G. Soyez, “A study of jet mass distributions with grooming”, *JHEP* **07** (2017) 132, arXiv:1704.02210 [hep-ph].
- [23] S. Marzani, L. Schunk, and G. Soyez, “The jet mass distribution after Soft Drop”, *Eur. Phys. J. C* **78** (2018) 96, arXiv:1712.05105 [hep-ph].
- [24] A. Kardos, A. J. Larkoski, and Z. Trócsányi, “Groomed jet mass at high precision”, *Phys. Lett. B* **809** (2020) 135704, arXiv:2002.00942 [hep-ph].
- [25] C. F. Berger, T. Kúcs, and G. F. Sterman, “Interjet energy flow/event shape correlations”, *Int. J. Mod. Phys. A* **18** (2003) 4159–4168, arXiv:hep-ph/0212343.
- [26] C. F. Berger, T. Kúcs, and G. F. Sterman, “Event shape/energy flow correlations”, *Phys. Rev. D* **68** (2003) 014012, arXiv:hep-ph/0303051.
- [27] C. F. Berger and L. Magnea, “Scaling of power corrections for angularities from dressed gluon exponentiation”, *Phys. Rev. D* **70** (2004) 094010, arXiv:hep-ph/0407024.

- [28] L. G. Almeida, S. J. Lee, G. Perez, G. F. Sterman, I. Sung, and J. Virzi, “Substructure of high- p_T jets at the LHC”, *Phys. Rev. D* **79** (2009) 074017, arXiv:0807.0234 [hep-ph].
- [29] A. J. Larkoski, J. Thaler, and W. J. Waalewijn, “Gaining (mutual) information about quark/gluon discrimination”, *JHEP* **11** (2014) 129, arXiv:1408.3122 [hep-ph].
- [30] C. F. Berger and G. F. Sterman, “Scaling rule for nonperturbative radiation in a class of event shapes”, *JHEP* **09** (2003) 058, arXiv:hep-ph/0307394.
- [31] E. Farhi, “Quantum Chromodynamics Test for Jets”, *Phys. Rev. Lett.* **39** (1977) 1587–1588.
- [32] Z.-B. Kang, K. Lee, and F. Ringer, “Jet angularity measurements for single inclusive jet production”, *JHEP* **04** (2018) 110, arXiv:1801.00790 [hep-ph].
- [33] S. Catani, G. Turnock, and B. Webber, “Jet broadening measures in e^+e^- annihilation”, *Phys. Lett. B* **295** (1992) 269–276.
- [34] ALICE Collaboration, S. Acharya *et al.*, “Medium modification of the shape of small-radius jets in central Pb–Pb collisions at $\sqrt{s_{NN}} = 2.76$ TeV”, *JHEP* **10** (2018) 139, arXiv:1807.06854 [nucl-ex].
- [35] ALICE Collaboration, S. Acharya *et al.*, “Measurements of the groomed and ungroomed jet angularities in pp collisions at $\sqrt{s} = 5.02$ TeV”, *JHEP* **05** (2022) 061, arXiv:2107.11303 [nucl-ex].
- [36] A. J. Larkoski, S. Marzani, G. Soyez, and J. Thaler, “Soft Drop”, *JHEP* **05** (2014) 146, arXiv:1402.2657 [hep-ph].
- [37] ALICE Collaboration, K. Aamodt *et al.*, “The ALICE experiment at the CERN LHC”, *JINST* **3** (2008) S08002.
- [38] ALICE Collaboration, B. Abelev *et al.*, “Performance of the ALICE experiment at the CERN LHC”, *Int. J. Mod. Phys. A* **29** (2014) 1430044, arXiv:1402.4476 [nucl-ex].
- [39] L. Evans and P. Bryant, “The CERN Large Hadron Collider: accelerator and experiments”, *JINST* **3** (2008) S08001.
- [40] ALICE Collaboration, E. Abbas *et al.*, “Performance of the ALICE VZERO system”, *JINST* **8** (2013) P10016, arXiv:1306.3130 [nucl-ex].
- [41] ALICE Collaboration, S. Acharya *et al.*, “Centrality determination in heavy-ion collisions.” CERN, 2018. <http://cds.cern.ch/record/2636623>.
- [42] ALICE Collaboration, J. Adam *et al.*, “Charged-particle multiplicities in proton-proton collisions at $\sqrt{s} = 0.9$ to 8 TeV”, *Eur. Phys. J. C* **77** (2017) 33.
- [43] ALICE Collaboration, S. Acharya *et al.*, “ALICE 2017 luminosity determination for pp collisions at $\sqrt{s} = 5$ TeV.” CERN, 2018. <http://cds.cern.ch/record/2648933>.
- [44] ALICE Collaboration, S. Acharya *et al.*, “ALICE luminosity determination for Pb–Pb collisions at $\sqrt{s_{NN}} = 5.02$ TeV”, *J. Inst.* **19** (2024) P02039, arXiv:2204.10148 [nucl-ex].
- [45] ALICE Collaboration, J. Alme *et al.*, “The ALICE TPC, a large 3-dimensional tracking device with fast readout for ultra-high multiplicity events”, *NIM A* **622** (2010) 316–367, arXiv:1001.1950 [physics.ins-det].

- [46] ALICE Collaboration, K. Aamod *et al.*, “Alignment of the ALICE Inner Tracking System with cosmic-ray tracks”, *JINST* **5** (2010) P03003, arXiv:1001.0502 [physics.ins-det].
- [47] ALICE Collaboration, S. Acharya *et al.*, “Measurement of charged jet cross section in pp collisions at $\sqrt{s} = 5.02$ TeV”, *Phys. Rev. D* **100** (2019) 092004, arXiv:1905.02536 [nucl-ex].
- [48] M. Cacciari, G. P. Salam, and G. Soyez, “FastJet user manual”, *Eur. Phys. J. C* **72** (2012) 1896, arXiv:1111.6097 [hep-ph].
- [49] M. Cacciari, G. P. Salam, and G. Soyez, “The anti- k_t jet clustering algorithm”, *JHEP* **04** (2008) 063, arXiv:0802.1189 [hep-ph].
- [50] H.-M. Chang, M. Procura, J. Thaler, and W. J. Waalewijn, “Calculating Track-Based Observables for the LHC”, *Phys. Rev. Lett.* **111** (2013) 102002, arXiv:1303.6637 [hep-ph].
- [51] ALICE Collaboration, B. Abelev *et al.*, “Measurement of event background fluctuations for charged particle jet reconstruction in Pb–Pb collisions at $\sqrt{s_{NN}} = 2.76$ TeV”, *JHEP* **03** (2012) 053, arXiv:1201.2423 [hep-ex].
- [52] P. Berta, M. Spousta, D. W. Miller, and R. Leitner, “Particle-level pileup subtraction for jets and jet shapes”, *JHEP* **06** (2014) 092, arXiv:1403.3108 [hep-ex].
- [53] Y. Dokshitzer, G. Leder, S. Moretti, and B. Webber, “Better jet clustering algorithms”, *JHEP* **08** (1997) 001.
- [54] J. Mulligan and M. Płoskoń, “Identifying groomed jet splittings in heavy-ion collisions”, *Phys. Rev. C* **102** (2020) 044913, arXiv:2006.01812 [hep-ph].
- [55] T. Sjöstrand *et al.*, “An introduction to PYTHIA 8.2”, *Comput. Phys. Commun.* **191** (2015) 159–177, arXiv:1410.3012 [hep-ph].
- [56] R. Brun, F. Bruyant, M. Maire, A. C. McPherson, and P. Zancarini, “GEANT 3: user’s guide Geant 3.10, Geant 3.11; rev. version.” CERN, 1987. <https://cds.cern.ch/record/1119728>.
- [57] G. D’Agostini, “A multidimensional unfolding method based on Bayes’ theorem”, *NIM A* **362** (1995) 487–498.
- [58] “RooUnfold.” <https://hepunix.rl.ac.uk/~adye/software/unfold/RooUnfold.html>.
- [59] ALICE Collaboration, S. Acharya *et al.*, “Supplemental material: Medium-induced modification of the groomed and ungroomed jet mass and angularities in Pb–Pb collisions at $\sqrt{s_{NN}} = 5.02$ TeV.” ALICE-PUBLIC-2024-004, 2024. <https://cds.cern.ch/record/2910744>. Public Note.
- [60] M. Bähr, *et al.*, “Herwig++ physics and manual”, *Eur. Phys. J. C* **58** (2008) 639–707, arXiv:0803.0883 [hep-ph].
- [61] J. Bellm *et al.*, “Herwig 7.0/Herwig++ 3.0 release note”, *Eur. Phys. J. C* **76** (2016) 196, arXiv:1512.01178 [hep-ph].
- [62] K. Zapp, “JEWEL 2.0.0: Directions for Use”, *Eur. Phys. J. C* **74** (2014) 2762, arXiv:1311.0048 [hep-ph].
- [63] J. H. Putschke *et al.*, “The JETSCAPE framework”, arXiv:1903.07706 [nucl-th].
- [64] A. Majumder, “Incorporating space-time within medium-modified jet-event generators”, *Phys. Rev. C* **88** (2013) 014909, arXiv:1301.5323 [nucl-th].

















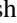


















- [65] Y. He, T. Luo, X.-N. Wang, and Y. Zhu, “Linear Boltzmann transport for jet propagation in the quark-gluon plasma: Elastic processes and medium recoil”, *Phys. Rev. C* **91** (2015) 054908, arXiv:1503.03313 [nucl-th].
- [66] J. Yan, S.-Y. Chen, W. Dai, B.-W. Zhang, and E.-K. Wang, “Medium modifications of girth distributions for inclusive jets and $Z^0 + \text{jet}$ in relativistic heavy-ion collisions at the LHC”, *Chin. Phys. C* **45** (2021) 024102, arXiv:2005.01093 [hep-ph].
- [67] P. Nason, “A New Method for Combining NLO QCD with Shower Monte Carlo Algorithms”, *JHEP* **11** (2004) 040, arXiv:hep-ph/0409146.
- [68] X. Guo and X.-N. Wang, “Multiple Scattering, Parton Energy Loss, and Modified Fragmentation Functions in Deeply Inelastic eA Scattering”, *Phys. Rev. Lett.* **85** (2000) 3591–3594, arXiv:hep-ph/0005044.
- [69] B.-W. Zhang and X.-N. Wang, “Multiple parton scattering in nuclei: beyond helicity amplitude approximation”, *Nucl. Phys. A* **720** (2003) 429–451, arXiv:hep-ph/0301195.
- [70] B.-W. Zhang, E. Wang, and X.-N. Wang, “Heavy quark energy loss in nuclear medium”, *Phys. Rev. Lett.* **93** (2004) 072301, arXiv:nucl-th/0309040.
- [71] A. Majumder, “Hard collinear gluon radiation and multiple scattering in a medium”, *Phys. Rev. D* **85** (2012) 014023, arXiv:0912.2987 [nucl-th].
- [72] J. Casalderrey-Solana, D. C. Gulhan, J. G. Milhano, D. Pablos, and K. Rajagopal, “A hybrid strong/weak coupling approach to jet quenching”, *JHEP* **10** (2014) 019, arXiv:1405.3864 [nucl-th].
- [73] F. D’Eramo, K. Rajagopal, and Y. Yin, “Molière scattering in quark-gluon plasma: finding point-like scatterers in a liquid”, *JHEP* **01** (2019) 172, arXiv:1808.03250 [hep-ph].

A The ALICE Collaboration

S. Acharya ¹²⁶, A. Agarwal ¹³⁴, G. Aglieri Rinella ³², L. Aglietta ²⁴, M. Agnello ²⁹, N. Agrawal ²⁵, Z. Ahammed ¹³⁴, S. Ahmad ¹⁵, S.U. Ahn ⁷¹, I. Ahuja ³⁶, A. Akindinov ¹⁴⁰, V. Akishina ³⁸, M. Al-Turany ⁹⁶, D. Aleksandrov ¹⁴⁰, B. Alessandro ⁵⁶, H.M. Alfanda ⁶, R. Alfaro Molina ⁶⁷, B. Ali ¹⁵, A. Alici ²⁵, N. Alizadehvandchali ¹¹⁵, A. Alkin ¹⁰³, J. Alme ²⁰, G. Alocco ^{24,52}, T. Alt ⁶⁴, A.R. Altamura ⁵⁰, I. Altsybeev ⁹⁴, J.R. Alvarado ⁴⁴, C.O.R. Alvarez ⁴⁴, M.N. Anaam ⁶, C. Andrei ⁴⁵, N. Andreou ¹¹⁴, A. Andronic ¹²⁵, E. Andronov ¹⁴⁰, V. Anguelov ⁹³, F. Antinori ⁵⁴, P. Antonioli ⁵¹, N. Apadula ⁷³, L. Aphecetche ¹⁰², H. Appelshäuser ⁶⁴, C. Arata ⁷², S. Arcelli ²⁵, R. Arnaldi ⁵⁶, J.G.M.C.A. Arneiro ¹⁰⁹, I.C. Arsene ¹⁹, M. Arslanok ¹³⁷, A. Augustinus ³², R. Averbeck ⁹⁶, D. Averyanov ¹⁴⁰, M.D. Azmi ¹⁵, H. Baba ¹²³, A. Badalà ⁵³, J. Bae ¹⁰³, Y. Bae ¹⁰³, Y.W. Baek ⁴⁰, X. Bai ¹¹⁹, R. Bailhache ⁶⁴, Y. Bailung ⁴⁸, R. Bala ⁹⁰, A. Balbino ²⁹, A. Baldisseri ¹²⁹, B. Balis ², Z. Banoo ⁹⁰, V. Barbasova ³⁶, F. Barile ³¹, L. Barioglio ⁵⁶, M. Barlou ⁷⁷, B. Barman ⁴¹, G.G. Barnaföldi ⁴⁶, L.S. Barnby ¹¹⁴, E. Barreau ¹⁰², V. Barret ¹²⁶, L. Barreto ¹⁰⁹, C. Bartels ¹¹⁸, K. Barth ³², E. Bartsch ⁶⁴, N. Bastid ¹²⁶, S. Basu ⁷⁴, G. Batigne ¹⁰², D. Battistini ⁹⁴, B. Batyunya ¹⁴¹, D. Bauri ⁴⁷, J.L. Bazo Alba ¹⁰⁰, I.G. Bearden ⁸², C. Beattie ¹³⁷, P. Becht ⁹⁶, D. Behera ⁴⁸, I. Belikov ¹²⁸, A.D.C. Bell Hechavarria ¹²⁵, F. Bellini ²⁵, R. Bellwied ¹¹⁵, S. Belokurova ¹⁴⁰, L.G.E. Beltran ¹⁰⁸, Y.A.V. Beltran ⁴⁴, G. Bencedi ⁴⁶, A. Bensaoula ¹¹⁵, S. Beole ²⁴, Y. Berdnikov ¹⁴⁰, A. Berdnikova ⁹³, L. Bergmann ⁹³, M.G. Besoiu ⁶³, L. Betev ³², P.P. Bhaduri ¹³⁴, A. Bhasin ⁹⁰, B. Bhattacharjee ⁴¹, L. Bianchi ²⁴, J. Bielčík ³⁴, J. Bielčíková ⁸⁵, A.P. Bigot ¹²⁸, A. Bilandzic ⁹⁴, G. Biro ⁴⁶, S. Biswas ⁴, N. Bize ¹⁰², J.T. Blair ¹⁰⁷, D. Blau ¹⁴⁰, M.B. Blidaru ⁹⁶, N. Bluhme ³⁸, C. Blume ⁶⁴, F. Bock ⁸⁶, T. Bodova ²⁰, J. Bok ¹⁶, L. Boldizsár ⁴⁶, M. Bombara ³⁶, P.M. Bond ³², G. Bonomi ^{133,55}, H. Borel ¹²⁹, A. Borissov ¹⁴⁰, A.G. Borquez Carcamo ⁹³, E. Botta ²⁴, Y.E.M. Bouziani ⁶⁴, L. Bratrud ⁶⁴, P. Braun-Munzinger ⁹⁶, M. Bregant ¹⁰⁹, M. Broz ³⁴, G.E. Bruno ^{95,31}, V.D. Buchakchiev ³⁵, M.D. Buckland ⁸⁴, D. Budnikov ¹⁴⁰, H. Buesching ⁶⁴, S. Bufalino ²⁹, P. Buhler ¹⁰¹, N. Burmasov ¹⁴⁰, Z. Buthelezi ^{68,122}, A. Bylinkin ²⁰, S.A. Bysiak ¹⁰⁶, J.C. Cabanillas Noris ¹⁰⁸, M.F.T. Cabrera ¹¹⁵, H. Caines ¹³⁷, A. Caliva ²⁸, E. Calvo Villar ¹⁰⁰, J.M.M. Camacho ¹⁰⁸, P. Camerini ²³, F.D.M. Canedo ¹⁰⁹, S.L. Cantway ¹³⁷, M. Carabas ¹¹², A.A. Carballo ³², F. Carnesecchi ³², R. Caron ¹²⁷, L.A.D. Carvalho ¹⁰⁹, J. Castillo Castellanos ¹²⁹, M. Castoldi ³², F. Catalano ³², S. Cattaruzzi ²³, R. Cerri ²⁴, I. Chakaberia ⁷³, P. Chakraborty ¹³⁵, S. Chandra ¹³⁴, S. Chapeland ³², M. Chartier ¹¹⁸, S. Chattopadhyay ¹³⁴, M. Chen ³⁹, T. Cheng ⁶, C. Cheshkov ¹²⁷, D. Chiappara ²⁷, V. Chibante Barroso ³², D.D. Chinellato ¹⁰¹, E.S. Chizzali ^{11,94}, J. Cho ⁵⁸, S. Cho ⁵⁸, P. Chochula ³², Z.A. Chochulska ¹³⁵, D. Choudhury ⁴¹, S. Choudhury ⁹⁸, P. Christakoglou ⁸³, C.H. Christensen ⁸², P. Christiansen ⁷⁴, T. Chujo ¹²⁴, M. Ciacco ²⁹, C. Cicalo ⁵², F. Cindolo ⁵¹, M.R. Ciupek ⁹⁶, G. Clai ^{III,51}, F. Colamaria ⁵⁰, J.S. Colburn ⁹⁹, D. Colella ³¹, A. Colelli ³¹, M. Colocci ²⁵, M. Concas ³², G. Conesa Balbastre ⁷², Z. Conesa del Valle ¹³⁰, G. Contin ²³, J.G. Contreras ³⁴, M.L. Coquet ¹⁰², P. Cortese ^{132,56}, M.R. Cosentino ¹¹¹, F. Costa ³², S. Costanza ^{21,55}, C. Cot ¹³⁰, P. Crochet ¹²⁶, M.M. Czarnynoga ¹³⁵, A. Dainese ⁵⁴, G. Dange ³⁸, M.C. Danisch ⁹³, A. Danu ⁶³, P. Das ^{32,79}, S. Das ⁴, A.R. Dash ¹²⁵, S. Dash ⁴⁷, A. De Caro ²⁸, G. de Cataldo ⁵⁰, J. de Cuveland ³⁸, A. De Falco ²², D. De Gruttola ²⁸, N. De Marco ⁵⁶, C. De Martin ²³, S. De Pasquale ²⁸, R. Deb ¹³³, R. Del Grande ⁹⁴, L. Dello Stritto ³², W. Deng ⁶, K.C. Devereaux ¹⁸, P. Dhankher ¹⁸, D. Di Bari ³¹, A. Di Mauro ³², B. Di Ruzza ¹³¹, B. Diab ¹²⁹, R.A. Diaz ^{141,7}, Y. Ding ⁶, J. Ditzel ⁶⁴, R. Divià ³², Ø. Djuvsland ²⁰, U. Dmitrieva ¹⁴⁰, A. Dobrin ⁶³, B. Dönigus ⁶⁴, J.M. Dubinski ¹³⁵, A. Dubla ⁹⁶, P. Dupieux ¹²⁶, N. Dzalaiova ¹³, T.M. Eder ¹²⁵, R.J. Ehlers ⁷³, F. Eisenhut ⁶⁴, R. Ejima ⁹¹, D. Elia ⁵⁰, B. Erasmus ¹⁰², F. Ercolessi ²⁵, B. Espagnon ¹³⁰, G. Eulisse ³², D. Evans ⁹⁹, S. Evdokimov ¹⁴⁰, L. Fabbietti ⁹⁴, M. Faggin ²³, J. Faivre ⁷², F. Fan ⁶, W. Fan ⁷³, A. Fantoni ⁴⁹, M. Fasel ⁸⁶, G. Feofilov ¹⁴⁰, A. Fernández Téllez ⁴⁴, L. Ferrandi ¹⁰⁹, M.B. Ferrer ³², A. Ferrero ¹²⁹, C. Ferrero ^{IV,56}, A. Ferretti ²⁴, V.J.G. Feuillard ⁹³, V. Filova ³⁴, D. Finogeev ¹⁴⁰, F.M. Fionda ⁵², E. Flatland ³², F. Flor ^{137,115}, A.N. Flores ¹⁰⁷, S. Foertsch ⁶⁸, I. Fokin ⁹³, S. Fokin ¹⁴⁰, U. Follo ^{IV,56}, E. Fragiaco ⁵⁷, E. Frajna ⁴⁶, U. Fuchs ³², N. Funicello ²⁸, C. Furget ⁷², A. Furs ¹⁴⁰, T. Fusayasu ⁹⁷, J.J. Gaardhøje ⁸², M. Gagliardi ²⁴, A.M. Gago ¹⁰⁰, T. Gahlaut ⁴⁷, C.D. Galvan ¹⁰⁸, S. Gami ⁷⁹, D.R. Gangadharan ¹¹⁵, P. Ganoti ⁷⁷, C. Garabatos ⁹⁶, J.M. Garcia ⁴⁴, T. García Chávez ⁴⁴, E. Garcia-Solis ³², C. Gargiulo ³², P. Gasik ⁹⁶, H.M. Gaur ³⁸, A. Gautam ¹¹⁷, M.B. Gay Ducati ⁶⁶, M. Germain ¹⁰², R.A. Gernhaeuser ⁹⁴, C. Ghosh ¹³⁴, M. Giacalone ⁵¹, G. Gioachin ²⁹, S.K. Giri ¹³⁴, P. Giubellino ^{96,56}, P. Giubilato ²⁷, A.M.C. Glaenger ¹²⁹, P. Glässel ⁹³, E. Glimos ¹²¹, D.J.Q. Goh ⁷⁵, V. Gonzalez ¹³⁶, P. Gordeev ¹⁴⁰, M. Gorgon ², K. Goswami ⁴⁸, S. Gotovac ³³, V. Grabski ⁶⁷, L.K. Graczykowski ¹³⁵, E. Grecka ⁸⁵, A. Grelli ⁵⁹, C. Grigoras ³², V. Grigoriev ¹⁴⁰, S. Grigoryan ^{141,1},

F. Grosa ³², J.F. Grosse-Oetringhaus ³², R. Grosso ⁹⁶, D. Grund ³⁴, N.A. Grunwald ⁹³, G.G. Guardiano ¹¹⁰, R. Guernane ⁷², M. Guilbaud ¹⁰², K. Gulbrandsen ⁸², J.J.W.K. Gumprecht ¹⁰¹, T. Gündem ⁶⁴, T. Gunji ¹²³, W. Guo ⁶, A. Gupta ⁹⁰, R. Gupta ⁹⁰, R. Gupta ⁴⁸, K. Gwizdziel ¹³⁵, L. Gyulai ⁴⁶, C. Hadjidakis ¹³⁰, F.U. Haider ⁹⁰, S. Haidlova ³⁴, M. Haldar ⁴, H. Hamagaki ⁷⁵, Y. Han ¹³⁹, B.G. Hanley ¹³⁶, R. Hannigan ¹⁰⁷, J. Hansen ⁷⁴, M.R. Haque ⁹⁶, J.W. Harris ¹³⁷, A. Harton ⁹, M.V. Hartung ⁶⁴, H. Hassan ¹¹⁶, D. Hatzifotiadou ⁵¹, P. Hauer ⁴², L.B. Havener ¹³⁷, E. Hellbär ³², H. Helstrup ³⁷, M. Hemmer ⁶⁴, T. Herman ³⁴, S.G. Hernandez ¹¹⁵, G. Herrera Corral ⁸, S. Herrmann ¹²⁷, K.F. Hetland ³⁷, B. Heybeck ⁶⁴, H. Hillemanns ³², B. Hippolyte ¹²⁸, I.P.M. Hobus ⁸³, F.W. Hoffmann ⁷⁰, B. Hofman ⁵⁹, M. Horst ⁹⁴, A. Horzyk ², Y. Hou ⁶, P. Hristov ³², P. Huhn ⁶⁴, L.M. Huhta ¹¹⁶, T.J. Humanic ⁸⁷, A. Hutson ¹¹⁵, D. Hutter ³⁸, M.C. Hwang ¹⁸, R. Ilkaev ¹⁴⁰, M. Inaba ¹²⁴, G.M. Innocenti ³², M. Ippolitov ¹⁴⁰, A. Isakov ⁸³, T. Isidori ¹¹⁷, M.S. Islam ^{47,98}, S. Iurchenko ¹⁴⁰, M. Ivanov ¹³, M. Ivanov ⁹⁶, V. Ivanov ¹⁴⁰, K.E. Iversen ⁷⁴, M. Jablonski ², B. Jacak ^{18,73}, N. Jacazio ²⁵, P.M. Jacobs ⁷³, S. Jadlovská ¹⁰⁵, J. Jadlovsky ¹⁰⁵, S. Jaelani ⁸¹, C. Jahnke ¹⁰⁹, M.J. Jakubowska ¹³⁵, M.A. Janik ¹³⁵, T. Janson ⁷⁰, S. Ji ¹⁶, S. Jia ¹⁰, T. Jiang ¹⁰, A.A.P. Jimenez ⁶⁵, F. Jonas ⁷³, D.M. Jones ¹¹⁸, J.M. Jowett ^{32,96}, J. Jung ⁶⁴, M. Jung ⁶⁴, A. Junique ³², A. Jusko ⁹⁹, J. Kaewjai ¹⁰⁴, P. Kalinak ⁶⁰, A. Kalweit ³², A. Karasu Uysal ¹³⁸, D. Karatovic ⁸⁸, N. Karatzenis ⁹⁹, O. Karavichev ¹⁴⁰, T. Karavicheva ¹⁴⁰, E. Karpechev ¹⁴⁰, M.J. Karwowska ¹³⁵, U. Kebschull ⁷⁰, M. Keil ³², B. Ketzer ⁴², J. Keul ⁶⁴, S.S. Khade ⁴⁸, A.M. Khan ¹¹⁹, S. Khan ¹⁵, A. Khanzadeev ¹⁴⁰, Y. Kharlov ¹⁴⁰, A. Khatun ¹¹⁷, A. Khuntia ³⁴, Z. Khuranova ⁶⁴, B. Kileng ³⁷, B. Kim ¹⁰³, C. Kim ¹⁶, D.J. Kim ¹¹⁶, D. Kim ¹⁰³, E.J. Kim ⁶⁹, J. Kim ¹³⁹, J. Kim ⁵⁸, J. Kim ^{32,69}, M. Kim ¹⁸, S. Kim ¹⁷, T. Kim ¹³⁹, K. Kimura ⁹¹, A. Kirkova ³⁵, S. Kirsch ⁶⁴, I. Kisel ³⁸, S. Kiselev ¹⁴⁰, A. Kisiel ¹³⁵, J.L. Klay ⁵, J. Klein ³², S. Klein ⁷³, C. Klein-Bösing ¹²⁵, M. Kleiner ⁶⁴, T. Klemenz ⁹⁴, A. Kluge ³², C. Kobdaj ¹⁰⁴, R. Kohara ¹²³, T. Kollegger ⁹⁶, A. Kondratyev ¹⁴¹, N. Kondratyeva ¹⁴⁰, J. König ⁶⁴, S.A. Königstorfer ⁹⁴, P.J. Konopka ³², G. Kornakov ¹³⁵, M. Korwieser ⁹⁴, S.D. Koryciak ², C. Koster ⁸³, A. Kotliarov ⁸⁵, N. Kovacic ⁸⁸, V. Kovalenko ¹⁴⁰, M. Kowalski ¹⁰⁶, V. Kozuharov ³⁵, G. Kozlov ³⁸, I. Králik ⁶⁰, A. Kravčáková ³⁶, L. Krcal ^{32,38}, M. Krivda ^{99,60}, F. Krizek ⁸⁵, K. Krizkova Gajdosova ³², C. Krug ⁶⁶, M. Krüger ⁶⁴, D.M. Krupova ³⁴, E. Kryshen ¹⁴⁰, V. Kučera ⁵⁸, C. Kuhn ¹²⁸, P.G. Kuijjer ⁸³, T. Kumaoka ¹²⁴, D. Kumar ¹³⁴, L. Kumar ⁸⁹, N. Kumar ⁸⁹, S. Kumar ⁵⁰, S. Kundu ³², P. Kurashvili ⁷⁸, A.B. Kurepin ¹⁴⁰, A. Kuryakin ¹⁴⁰, S. Kushpil ⁸⁵, V. Kuskov ¹⁴⁰, M. Kutyla ¹³⁵, A. Kuznetsov ¹⁴¹, M.J. Kweon ⁵⁸, Y. Kwon ¹³⁹, S.L. La Pointe ³⁸, P. La Rocca ²⁶, A. Lakrathok ¹⁰⁴, M. Lamanna ³², A.R. Landou ⁷², R. Langoy ¹²⁰, P. Larionov ³², E. Laudi ³², L. Lautner ⁹⁴, R.A.N. Laveaga ¹⁰⁸, R. Lavicka ¹⁰¹, R. Lea ^{133,55}, H. Lee ¹⁰³, I. Legrand ⁴⁵, G. Legras ¹²⁵, J. Lehrbach ³⁸, A.M. Lejeune ³⁴, T.M. Lelek ², R.C. Lemmon ^{1,84}, I. León Monzón ¹⁰⁸, M.M. Lesch ⁹⁴, E.D. Lesser ¹⁸, P. Lévai ⁴⁶, M. Li ⁶, P. Li ¹⁰, X. Li ¹⁰, B.E. Liang-gilman ¹⁸, J. Lien ¹²⁰, R. Lietava ⁹⁹, I. Likmeta ¹¹⁵, B. Lim ²⁴, H. Lim ¹⁶, S.H. Lim ¹⁶, V. Lindenstruth ³⁸, C. Lippmann ⁹⁶, D. Liskova ¹⁰⁵, D.H. Liu ⁶, J. Liu ¹¹⁸, G.S.S. Liveraro ¹¹⁰, I.M. Lofnes ²⁰, C. Loizides ⁸⁶, S. Lokos ¹⁰⁶, J. Lömker ⁵⁹, X. Lopez ¹²⁶, E. López Torres ⁷, C. Lotteau ¹²⁷, P. Lu ^{96,119}, Z. Lu ¹⁰, F.V. Lugo ⁶⁷, J.R. Luhder ¹²⁵, G. Luparello ⁵⁷, Y.G. Ma ³⁹, M. Mager ³², A. Maire ¹²⁸, E.M. Majerz ², M.V. Makariev ³⁵, M. Malaev ¹⁴⁰, G. Malfattore ²⁵, N.M. Malik ⁹⁰, S.K. Malik ⁹⁰, D. Mallick ¹³⁰, N. Mallick ^{116,48}, G. Mandaglio ^{30,53}, S.K. Mandal ⁷⁸, A. Manea ⁶³, V. Manko ¹⁴⁰, F. Manso ¹²⁶, V. Manzari ⁵⁰, Y. Mao ⁶, R.W. Marcjan ², G.V. Margagliotti ²³, A. Margotti ⁵¹, A. Marín ⁹⁶, C. Markert ¹⁰⁷, C.F.B. Marquez ³¹, P. Martinengo ³², M.I. Martínez ⁴⁴, G. Martínez García ¹⁰², M.P.P. Martins ¹⁰⁹, S. Masciocchi ⁹⁶, M. Masera ²⁴, A. Masoni ⁵², L. Massacrier ¹³⁰, O. Massen ⁵⁹, A. Mastroserio ^{131,50}, S. Mattiazzo ²⁷, A. Matyja ¹⁰⁶, F. Mazzaschi ^{32,24}, M. Mazzilli ¹¹⁵, Y. Melikyan ⁴³, M. Melo ¹⁰⁹, A. Menchaca-Rocha ⁶⁷, J.E.M. Mendez ⁶⁵, E. Meninno ¹⁰¹, A.S. Menon ¹¹⁵, M.W. Menzel ^{32,93}, M. Meres ¹³, L. Micheletti ³², D. Mihai ¹¹², D.L. Mihaylov ⁹⁴, K. Mikhaylov ^{141,140}, N. Minafra ¹¹⁷, D. Miśkowiec ⁹⁶, A. Modak ¹³³, B. Mohanty ⁷⁹, M. Mohisin Khan ^{V,15}, M.A. Molander ⁴³, M.M. Mondal ⁷⁹, S. Monira ¹³⁵, C. Mordasini ¹¹⁶, D.A. Moreira De Godoy ¹²⁵, I. Morozov ¹⁴⁰, A. Morsch ³², T. Mrnjavac ³², V. Muccifora ⁴⁹, S. Muhuri ¹³⁴, J.D. Mulligan ⁷³, A. Mulliri ²², M.G. Munhoz ¹⁰⁹, R.H. Munzer ⁶⁴, H. Murakami ¹²³, S. Murray ¹¹³, L. Musa ³², J. Musinsky ⁶⁰, J.W. Myrcha ¹³⁵, B. Naik ¹²², A.I. Nambrath ¹⁸, B.K. Nandi ⁴⁷, R. Nania ⁵¹, E. Nappi ⁵⁰, A.F. Nassirpour ¹⁷, V. Nastase ¹¹², A. Nath ⁹³, S. Nath ¹³⁴, C. Nattrass ¹²¹, M.N. Naydenov ³⁵, A. Neagu ¹⁹, A. Negru ¹¹², E. Nekrasova ¹⁴⁰, L. Nellen ⁶⁵, R. Nepeivoda ⁷⁴, S. Nese ¹⁹, N. Nicassio ⁵⁰, B.S. Nielsen ⁸², E.G. Nielsen ⁸², S. Nikolaev ¹⁴⁰, V. Nikulin ¹⁴⁰, F. Noferini ⁵¹, S. Noh ¹², P. Nomokonov ¹⁴¹, J. Norman ¹¹⁸, N. Novitzky ⁸⁶, P. Nowakowski ¹³⁵, A. Nyanin ¹⁴⁰, J. Nystrand ²⁰, S. Oh ¹⁷, A. Ohlson ⁷⁴, V.A. Okorokov ¹⁴⁰, J. Oleniacz ¹³⁵, A. Onnerstad ¹¹⁶, C. Oppedisano ⁵⁶, A. Ortiz

Velasquez ⁶⁵, J. Otwinowski ¹⁰⁶, M. Oya ⁹¹, K. Oyama ⁷⁵, S. Padhan ⁴⁷, D. Pagano ^{133,55}, G. Paic ⁶⁵,
 S. Paisano-Guzmán ⁴⁴, A. Palasciano ⁵⁰, I. Panasenko ⁷⁴, S. Panebianco ¹²⁹, C. Pantouvakis ²⁷,
 H. Park ¹²⁴, J. Park ¹²⁴, S. Park ¹⁰³, J.E. Parkkila ³², Y. Patley ⁴⁷, R.N. Patra ⁵⁰, B. Paul ¹³⁴, H. Pei ⁶,
 T. Peitzmann ⁵⁹, X. Peng ¹¹, M. Pennisi ²⁴, S. Perciballi ²⁴, D. Peresunko ¹⁴⁰, G.M. Perez ⁷,
 Y. Pestov ¹⁴⁰, M.T. Petersen ⁸², V. Petrov ¹⁴⁰, M. Petrovici ⁴⁵, S. Piano ⁵⁷, M. Pikna ¹³, P. Pillot ¹⁰²,
 O. Pinazza ^{51,32}, L. Pinsky ¹¹⁵, C. Pinto ⁹⁴, S. Pisano ⁴⁹, M. Płoskoń ⁷³, M. Planinic ⁸⁸, D.K. Plociennik ²,
 M.G. Poghosyan ⁸⁶, B. Polichtchouk ¹⁴⁰, S. Politano ²⁹, N. Poljak ⁸⁸, A. Pop ⁴⁵,
 S. Porteboeuf-Houssais ¹²⁶, V. Pozdniakov ^{1,141}, I.Y. Pozos ⁴⁴, K.K. Pradhan ⁴⁸, S.K. Prasad ⁴,
 S. Prasad ⁴⁸, R. Preghenella ⁵¹, F. Prino ⁵⁶, C.A. Pruneau ¹³⁶, I. Pshenichnov ¹⁴⁰, M. Puccio ³²,
 S. Pucillo ²⁴, S. Qiu ⁸³, L. Quaglia ²⁴, A.M.K. Radhakrishnan ⁴⁸, S. Ragoni ¹⁴, A. Rai ¹³⁷,
 A. Rakotozafindrabe ¹²⁹, L. Ramello ^{132,56}, M. Rasa ²⁶, S.S. Räsänen ⁴³, R. Rath ⁵¹, M.P. Rauch ²⁰,
 I. Ravasenga ³², K.F. Read ^{86,121}, C. Reckziegel ¹¹¹, A.R. Redelbach ³⁸, K. Redlich ^{VI,78},
 C.A. Reetz ⁹⁶, H.D. Regules-Medel ⁴⁴, A. Rehman ²⁰, F. Reidt ³², H.A. Reme-Ness ³⁷, K. Reygiers ⁹³,
 A. Riabov ¹⁴⁰, V. Riabov ¹⁴⁰, R. Ricci ²⁸, M. Richter ²⁰, A.A. Riedel ⁹⁴, W. Riegler ³²,
 A.G. Riffero ²⁴, M. Rignanese ²⁷, C. Ripoli ²⁸, C. Ristea ⁶³, M.V. Rodriguez ³², M. Rodríguez
 Cahuantzi ⁴⁴, S.A. Rodríguez Ramírez ⁴⁴, K. Røed ¹⁹, R. Rogalev ¹⁴⁰, E. Rogochaya ¹⁴¹,
 T.S. Rogoschinski ⁶⁴, D. Rohr ³², D. Röhrich ²⁰, S. Rojas Torres ³⁴, P.S. Rokita ¹³⁵, G. Romanenko ²⁵,
 F. Ronchetti ³², E.D. Rosas ⁶⁵, K. Roslon ¹³⁵, A. Rossi ⁵⁴, A. Roy ⁴⁸, S. Roy ⁴⁷, N. Rubini ^{51,25},
 J.A. Rudolph ⁸³, D. Ruggiano ¹³⁵, R. Rui ²³, P.G. Russek ², R. Russo ⁸³, A. Rustamov ⁸⁰,
 E. Ryabinkin ¹⁴⁰, Y. Ryabov ¹⁴⁰, A. Rybicki ¹⁰⁶, J. Ryu ¹⁶, W. Rzesza ¹³⁵, B. Sabiu ⁵¹, S. Sadovsky ¹⁴⁰,
 J. Saetre ²⁰, S. Saha ⁷⁹, B. Sahoo ⁴⁸, R. Sahoo ⁴⁸, S. Sahoo ⁶¹, D. Sahu ⁴⁸, P.K. Sahu ⁶¹, J. Saini ¹³⁴,
 K. Sajdakova ³⁶, S. Sakai ¹²⁴, M.P. Salvan ⁹⁶, S. Sambyal ⁹⁰, D. Samitz ¹⁰¹, I. Sanna ^{32,94},
 T.B. Saramela ¹⁰⁹, D. Sarkar ⁸², P. Sarma ⁴¹, V. Sarritzu ²², V.M. Sarti ⁹⁴, M.H.P. Sas ³², S. Sawan ⁷⁹,
 E. Scapparone ⁵¹, J. Schambach ⁸⁶, H.S. Scheid ⁶⁴, C. Schiaua ⁴⁵, R. Schicker ⁹³, F. Schlepfer ⁹³,
 A. Schmah ⁹⁶, C. Schmidt ⁹⁶, M.O. Schmidt ³², M. Schmidt ⁹², N.V. Schmidt ⁸⁶, A.R. Schmier ¹²¹,
 R. Schotter ^{101,128}, A. Schröter ³⁸, J. Schukraft ³², K. Schweda ⁹⁶, G. Scioli ²⁵, E. Scomparin ⁵⁶,
 J.E. Seger ¹⁴, Y. Sekiguchi ¹²³, D. Sekihata ¹²³, M. Selina ⁸³, I. Selyuzhenkov ⁹⁶, S. Senyukov ¹²⁸,
 J.J. Seo ⁹³, D. Serebryakov ¹⁴⁰, L. Serkin ^{VII,65}, L. Šerkšnytė ⁹⁴, A. Sevcenco ⁶³, T.J. Shaba ⁶⁸,
 A. Shabetai ¹⁰², R. Shahoyan ³², A. Shangaraev ¹⁴⁰, B. Sharma ⁹⁰, D. Sharma ⁴⁷, H. Sharma ⁵⁴,
 M. Sharma ⁹⁰, S. Sharma ⁷⁵, S. Sharma ⁹⁰, U. Sharma ⁹⁰, A. Shatat ¹³⁰, O. Sheibani ^{136,115},
 K. Shigaki ⁹¹, M. Shimomura ⁷⁶, J. Shin ¹², S. Shirinkin ¹⁴⁰, Q. Shou ³⁹, Y. Sibiriak ¹⁴⁰, S. Siddhanta ⁵²,
 T. Siemiarzuk ⁷⁸, T.F. Silva ¹⁰⁹, D. Silvermyr ⁷⁴, T. Simantathammakul ¹⁰⁴, R. Simeonov ³⁵, B. Singh ⁹⁰,
 B. Singh ⁹⁴, K. Singh ⁴⁸, R. Singh ⁷⁹, R. Singh ⁹⁰, R. Singh ^{54,96}, S. Singh ¹⁵, V.K. Singh ¹³⁴,
 V. Singhal ¹³⁴, T. Sinha ⁹⁸, B. Sitar ¹³, M. Sitta ^{132,56}, T.B. Skaali ¹⁹, G. Skorodumovs ⁹³,
 N. Smirnov ¹³⁷, R.J.M. Snellings ⁵⁹, E.H. Solheim ¹⁹, C. Sonnabend ^{32,96}, J.M. Sonneveld ⁸³,
 F. Soramel ²⁷, A.B. Soto-hernandez ⁸⁷, R. Spijkers ⁸³, I. Sputowska ¹⁰⁶, J. Staa ⁷⁴, J. Stachel ⁹³,
 I. Stan ⁶³, P.J. Steffanic ¹²¹, T. Stellhorn ¹²⁵, S.F. Stiefelmaier ⁹³, D. Stocco ¹⁰², I. Storehaug ¹⁹,
 N.J. Strangmann ⁶⁴, P. Stratmann ¹²⁵, S. Strazzi ²⁵, A. Sturniolo ^{30,53}, C.P. Stylianidis ⁸³,
 A.A.P. Suaide ¹⁰⁹, C. Suire ¹³⁰, A. Suiu ^{32,112}, M. Sukhanov ¹⁴⁰, M. Suljic ³², R. Sultanov ¹⁴⁰,
 V. Sumberia ⁹⁰, S. Sumowidagdo ⁸¹, L.H. Tabares ⁷, S.F. Taghavi ⁹⁴, J. Takahashi ¹¹⁰, G.J. Tambave ⁷⁹,
 S. Tang ⁶, Z. Tang ¹¹⁹, J.D. Tapia Takaki ¹¹⁷, N. Tapus ¹¹², L.A. Tarasovicova ³⁶, M.G. Tarzila ⁴⁵,
 A. Tauro ³², A. Tavira García ¹³⁰, G. Tejeda Muñoz ⁴⁴, L. Terlizzi ²⁴, C. Terrevoli ⁵⁰, S. Thakur ⁴,
 M. Thogersen ¹⁹, D. Thomas ¹⁰⁷, A. Tikhonov ¹⁴⁰, N. Tiltmann ^{32,125}, A.R. Timmins ¹¹⁵, M. Tkacik ¹⁰⁵,
 T. Tkacik ¹⁰⁵, A. Toia ⁶⁴, R. Tokumoto ⁹¹, S. Tomassini ²⁵, K. Tomohiro ⁹¹, N. Topilskaya ¹⁴⁰,
 M. Toppi ⁴⁹, V.V. Torres ¹⁰², A.G. Torres Ramos ³¹, A. Trifiró ^{30,53}, T. Triloki ⁹⁵, A.S. Triolo ^{32,30,53},
 S. Tripathy ³², T. Tripathy ⁴⁷, S. Trogolo ²⁴, V. Trubnikov ³, W.H. Trzaska ¹¹⁶, T.P. Trzcinski ¹³⁵,
 C. Tzolanta ¹⁹, R. Tu ³⁹, A. Tumkin ¹⁴⁰, R. Turrisi ⁵⁴, T.S. Tveter ¹⁹, K. Ullaland ²⁰, B. Ulukutlu ⁹⁴,
 S. Upadhyaya ¹⁰⁶, A. Uras ¹²⁷, G.L. Usai ²², M. Vala ³⁶, N. Valle ⁵⁵, L.V.R. van Doremalen ⁵⁹, M. van
 Leeuwen ⁸³, C.A. van Veen ⁹³, R.J.G. van Weelden ⁸³, P. Vande Vyvre ³², D. Varga ⁴⁶, Z. Varga ^{137,46},
 P. Vargas Torres ⁶⁵, M. Vasileiou ⁷⁷, A. Vasiliev ^{I,140}, O. Vázquez Doce ⁴⁹, O. Vazquez Rueda ¹¹⁵,
 V. Vechernin ¹⁴⁰, E. Vercellin ²⁴, R. Verma ⁴⁷, R. Vértesi ⁴⁶, M. Verweij ⁵⁹, L. Vickovic ³³,
 Z. Vilakazi ¹²², O. Villalobos Baillie ⁹⁹, A. Villani ²³, A. Vinogradov ¹⁴⁰, T. Virgili ²⁸, M.M.O. Virta ¹¹⁶,
 A. Vodopyanov ¹⁴¹, B. Volkel ³², M.A. Völkl ⁹³, S.A. Voloshin ¹³⁶, G. Volpe ³¹, B. von Haller ³²,
 I. Vorobyev ³², N. Vozniuk ¹⁴⁰, J. Vrláková ³⁶, J. Wan ³⁹, C. Wang ³⁹, D. Wang ³⁹, Y. Wang ³⁹,
 Y. Wang ⁶, Z. Wang ³⁹, A. Wegrzynek ³², F.T. Weiglhofer ³⁸, S.C. Wenzel ³², J.P. Wessels ¹²⁵,
 P.K. Wiacek ², J. Wiechula ⁶⁴, J. Wikne ¹⁹, G. Wilk ⁷⁸, J. Wilkinson ⁹⁶, G.A. Willems ¹²⁵,

B. Windelband ⁹³, M. Winn ¹²⁹, J.R. Wright ¹⁰⁷, W. Wu³⁹, Y. Wu ¹¹⁹, Z. Xiong¹¹⁹, R. Xu ⁶,
A. Yadav ⁴², A.K. Yadav ¹³⁴, Y. Yamaguchi ⁹¹, S. Yang²⁰, S. Yano ⁹¹, E.R. Yeats¹⁸, Z. Yin ⁶,
I.-K. Yoo ¹⁶, J.H. Yoon ⁵⁸, H. Yu¹², S. Yuan²⁰, A. Yuncu ⁹³, V. Zaccolo ²³, C. Zampolli ³²,
F. Zanone ⁹³, N. Zardoshti ³², A. Zarochentsev ¹⁴⁰, P. Závada ⁶², N. Zaviyalov¹⁴⁰, M. Zhalov ¹⁴⁰,
B. Zhang ^{93,6}, C. Zhang ¹²⁹, L. Zhang ³⁹, M. Zhang ^{126,6}, M. Zhang ⁶, S. Zhang ³⁹, X. Zhang ⁶,
Y. Zhang¹¹⁹, Z. Zhang ⁶, M. Zhao ¹⁰, V. Zhrebchevskii ¹⁴⁰, Y. Zhi¹⁰, D. Zhou ⁶, Y. Zhou ⁸²,
J. Zhu ^{54,6}, S. Zhu¹¹⁹, Y. Zhu⁶, S.C. Zugravel ⁵⁶, N. Zurlo ^{133,55}

Affiliation Notes

^I Deceased

^{II} Also at: Max-Planck-Institut für Physik, Munich, Germany

^{III} Also at: Italian National Agency for New Technologies, Energy and Sustainable Economic Development (ENEA), Bologna, Italy

^{IV} Also at: Dipartimento DET del Politecnico di Torino, Turin, Italy

^V Also at: Department of Applied Physics, Aligarh Muslim University, Aligarh, India

^{VI} Also at: Institute of Theoretical Physics, University of Wrocław, Poland

^{VII} Also at: Facultad de Ciencias, Universidad Nacional Autónoma de México, Mexico City, Mexico

Collaboration Institutes

¹ A.I. Alikhanyan National Science Laboratory (Yerevan Physics Institute) Foundation, Yerevan, Armenia

² AGH University of Krakow, Cracow, Poland

³ Bogolyubov Institute for Theoretical Physics, National Academy of Sciences of Ukraine, Kiev, Ukraine

⁴ Bose Institute, Department of Physics and Centre for Astroparticle Physics and Space Science (CAPSS), Kolkata, India

⁵ California Polytechnic State University, San Luis Obispo, California, United States

⁶ Central China Normal University, Wuhan, China

⁷ Centro de Aplicaciones Tecnológicas y Desarrollo Nuclear (CEADEN), Havana, Cuba

⁸ Centro de Investigación y de Estudios Avanzados (CINVESTAV), Mexico City and Mérida, Mexico

⁹ Chicago State University, Chicago, Illinois, United States

¹⁰ China Institute of Atomic Energy, Beijing, China

¹¹ China University of Geosciences, Wuhan, China

¹² Chungbuk National University, Cheongju, Republic of Korea

¹³ Comenius University Bratislava, Faculty of Mathematics, Physics and Informatics, Bratislava, Slovak Republic

¹⁴ Creighton University, Omaha, Nebraska, United States

¹⁵ Department of Physics, Aligarh Muslim University, Aligarh, India

¹⁶ Department of Physics, Pusan National University, Pusan, Republic of Korea

¹⁷ Department of Physics, Sejong University, Seoul, Republic of Korea

¹⁸ Department of Physics, University of California, Berkeley, California, United States

¹⁹ Department of Physics, University of Oslo, Oslo, Norway

²⁰ Department of Physics and Technology, University of Bergen, Bergen, Norway

²¹ Dipartimento di Fisica, Università di Pavia, Pavia, Italy

²² Dipartimento di Fisica dell'Università and Sezione INFN, Cagliari, Italy

²³ Dipartimento di Fisica dell'Università and Sezione INFN, Trieste, Italy

²⁴ Dipartimento di Fisica dell'Università and Sezione INFN, Turin, Italy

²⁵ Dipartimento di Fisica e Astronomia dell'Università and Sezione INFN, Bologna, Italy

²⁶ Dipartimento di Fisica e Astronomia dell'Università and Sezione INFN, Catania, Italy

²⁷ Dipartimento di Fisica e Astronomia dell'Università and Sezione INFN, Padova, Italy

²⁸ Dipartimento di Fisica 'E.R. Caianiello' dell'Università and Gruppo Collegato INFN, Salerno, Italy

²⁹ Dipartimento DISAT del Politecnico and Sezione INFN, Turin, Italy

³⁰ Dipartimento di Scienze MIIFT, Università di Messina, Messina, Italy

³¹ Dipartimento Interateneo di Fisica 'M. Merlin' and Sezione INFN, Bari, Italy

³² European Organization for Nuclear Research (CERN), Geneva, Switzerland

³³ Faculty of Electrical Engineering, Mechanical Engineering and Naval Architecture, University of Split, Split, Croatia

- ³⁴ Faculty of Nuclear Sciences and Physical Engineering, Czech Technical University in Prague, Prague, Czech Republic
- ³⁵ Faculty of Physics, Sofia University, Sofia, Bulgaria
- ³⁶ Faculty of Science, P.J. Šafárik University, Košice, Slovak Republic
- ³⁷ Faculty of Technology, Environmental and Social Sciences, Bergen, Norway
- ³⁸ Frankfurt Institute for Advanced Studies, Johann Wolfgang Goethe-Universität Frankfurt, Frankfurt, Germany
- ³⁹ Fudan University, Shanghai, China
- ⁴⁰ Gangneung-Wonju National University, Gangneung, Republic of Korea
- ⁴¹ Gauhati University, Department of Physics, Guwahati, India
- ⁴² Helmholtz-Institut für Strahlen- und Kernphysik, Rheinische Friedrich-Wilhelms-Universität Bonn, Bonn, Germany
- ⁴³ Helsinki Institute of Physics (HIP), Helsinki, Finland
- ⁴⁴ High Energy Physics Group, Universidad Autónoma de Puebla, Puebla, Mexico
- ⁴⁵ Horia Hulubei National Institute of Physics and Nuclear Engineering, Bucharest, Romania
- ⁴⁶ HUN-REN Wigner Research Centre for Physics, Budapest, Hungary
- ⁴⁷ Indian Institute of Technology Bombay (IIT), Mumbai, India
- ⁴⁸ Indian Institute of Technology Indore, Indore, India
- ⁴⁹ INFN, Laboratori Nazionali di Frascati, Frascati, Italy
- ⁵⁰ INFN, Sezione di Bari, Bari, Italy
- ⁵¹ INFN, Sezione di Bologna, Bologna, Italy
- ⁵² INFN, Sezione di Cagliari, Cagliari, Italy
- ⁵³ INFN, Sezione di Catania, Catania, Italy
- ⁵⁴ INFN, Sezione di Padova, Padova, Italy
- ⁵⁵ INFN, Sezione di Pavia, Pavia, Italy
- ⁵⁶ INFN, Sezione di Torino, Turin, Italy
- ⁵⁷ INFN, Sezione di Trieste, Trieste, Italy
- ⁵⁸ Inha University, Incheon, Republic of Korea
- ⁵⁹ Institute for Gravitational and Subatomic Physics (GRASP), Utrecht University/Nikhef, Utrecht, Netherlands
- ⁶⁰ Institute of Experimental Physics, Slovak Academy of Sciences, Košice, Slovak Republic
- ⁶¹ Institute of Physics, Homi Bhabha National Institute, Bhubaneswar, India
- ⁶² Institute of Physics of the Czech Academy of Sciences, Prague, Czech Republic
- ⁶³ Institute of Space Science (ISS), Bucharest, Romania
- ⁶⁴ Institut für Kernphysik, Johann Wolfgang Goethe-Universität Frankfurt, Frankfurt, Germany
- ⁶⁵ Instituto de Ciencias Nucleares, Universidad Nacional Autónoma de México, Mexico City, Mexico
- ⁶⁶ Instituto de Física, Universidade Federal do Rio Grande do Sul (UFRGS), Porto Alegre, Brazil
- ⁶⁷ Instituto de Física, Universidad Nacional Autónoma de México, Mexico City, Mexico
- ⁶⁸ iThemba LABS, National Research Foundation, Somerset West, South Africa
- ⁶⁹ Jeonbuk National University, Jeonju, Republic of Korea
- ⁷⁰ Johann-Wolfgang-Goethe Universität Frankfurt Institut für Informatik, Fachbereich Informatik und Mathematik, Frankfurt, Germany
- ⁷¹ Korea Institute of Science and Technology Information, Daejeon, Republic of Korea
- ⁷² Laboratoire de Physique Subatomique et de Cosmologie, Université Grenoble-Alpes, CNRS-IN2P3, Grenoble, France
- ⁷³ Lawrence Berkeley National Laboratory, Berkeley, California, United States
- ⁷⁴ Lund University Department of Physics, Division of Particle Physics, Lund, Sweden
- ⁷⁵ Nagasaki Institute of Applied Science, Nagasaki, Japan
- ⁷⁶ Nara Women's University (NWU), Nara, Japan
- ⁷⁷ National and Kapodistrian University of Athens, School of Science, Department of Physics, Athens, Greece
- ⁷⁸ National Centre for Nuclear Research, Warsaw, Poland
- ⁷⁹ National Institute of Science Education and Research, Homi Bhabha National Institute, Jatni, India
- ⁸⁰ National Nuclear Research Center, Baku, Azerbaijan
- ⁸¹ National Research and Innovation Agency - BRIN, Jakarta, Indonesia
- ⁸² Niels Bohr Institute, University of Copenhagen, Copenhagen, Denmark
- ⁸³ Nikhef, National institute for subatomic physics, Amsterdam, Netherlands
- ⁸⁴ Nuclear Physics Group, STFC Daresbury Laboratory, Daresbury, United Kingdom
- ⁸⁵ Nuclear Physics Institute of the Czech Academy of Sciences, Husinec-Řež, Czech Republic

- ⁸⁶ Oak Ridge National Laboratory, Oak Ridge, Tennessee, United States
- ⁸⁷ Ohio State University, Columbus, Ohio, United States
- ⁸⁸ Physics department, Faculty of science, University of Zagreb, Zagreb, Croatia
- ⁸⁹ Physics Department, Panjab University, Chandigarh, India
- ⁹⁰ Physics Department, University of Jammu, Jammu, India
- ⁹¹ Physics Program and International Institute for Sustainability with Knotted Chiral Meta Matter (WPI-SKCM²), Hiroshima University, Hiroshima, Japan
- ⁹² Physikalisches Institut, Eberhard-Karls-Universität Tübingen, Tübingen, Germany
- ⁹³ Physikalisches Institut, Ruprecht-Karls-Universität Heidelberg, Heidelberg, Germany
- ⁹⁴ Physik Department, Technische Universität München, Munich, Germany
- ⁹⁵ Politecnico di Bari and Sezione INFN, Bari, Italy
- ⁹⁶ Research Division and ExtreMe Matter Institute EMMI, GSI Helmholtzzentrum für Schwerionenforschung GmbH, Darmstadt, Germany
- ⁹⁷ Saga University, Saga, Japan
- ⁹⁸ Saha Institute of Nuclear Physics, Homi Bhabha National Institute, Kolkata, India
- ⁹⁹ School of Physics and Astronomy, University of Birmingham, Birmingham, United Kingdom
- ¹⁰⁰ Sección Física, Departamento de Ciencias, Pontificia Universidad Católica del Perú, Lima, Peru
- ¹⁰¹ Stefan Meyer Institut für Subatomare Physik (SMI), Vienna, Austria
- ¹⁰² SUBATECH, IMT Atlantique, Nantes Université, CNRS-IN2P3, Nantes, France
- ¹⁰³ Sungkyunkwan University, Suwon City, Republic of Korea
- ¹⁰⁴ Suranaree University of Technology, Nakhon Ratchasima, Thailand
- ¹⁰⁵ Technical University of Košice, Košice, Slovak Republic
- ¹⁰⁶ The Henryk Niewodniczanski Institute of Nuclear Physics, Polish Academy of Sciences, Cracow, Poland
- ¹⁰⁷ The University of Texas at Austin, Austin, Texas, United States
- ¹⁰⁸ Universidad Autónoma de Sinaloa, Culiacán, Mexico
- ¹⁰⁹ Universidade de São Paulo (USP), São Paulo, Brazil
- ¹¹⁰ Universidade Estadual de Campinas (UNICAMP), Campinas, Brazil
- ¹¹¹ Universidade Federal do ABC, Santo Andre, Brazil
- ¹¹² Universitatea Nationala de Stiinta si Tehnologie Politehnica Bucuresti, Bucharest, Romania
- ¹¹³ University of Cape Town, Cape Town, South Africa
- ¹¹⁴ University of Derby, Derby, United Kingdom
- ¹¹⁵ University of Houston, Houston, Texas, United States
- ¹¹⁶ University of Jyväskylä, Jyväskylä, Finland
- ¹¹⁷ University of Kansas, Lawrence, Kansas, United States
- ¹¹⁸ University of Liverpool, Liverpool, United Kingdom
- ¹¹⁹ University of Science and Technology of China, Hefei, China
- ¹²⁰ University of South-Eastern Norway, Kongsberg, Norway
- ¹²¹ University of Tennessee, Knoxville, Tennessee, United States
- ¹²² University of the Witwatersrand, Johannesburg, South Africa
- ¹²³ University of Tokyo, Tokyo, Japan
- ¹²⁴ University of Tsukuba, Tsukuba, Japan
- ¹²⁵ Universität Münster, Institut für Kernphysik, Münster, Germany
- ¹²⁶ Université Clermont Auvergne, CNRS/IN2P3, LPC, Clermont-Ferrand, France
- ¹²⁷ Université de Lyon, CNRS/IN2P3, Institut de Physique des 2 Infinis de Lyon, Lyon, France
- ¹²⁸ Université de Strasbourg, CNRS, IPHC UMR 7178, F-67000 Strasbourg, France, Strasbourg, France
- ¹²⁹ Université Paris-Saclay, Centre d'Etudes de Saclay (CEA), IRFU, Département de Physique Nucléaire (DPHN), Saclay, France
- ¹³⁰ Université Paris-Saclay, CNRS/IN2P3, IJCLab, Orsay, France
- ¹³¹ Università degli Studi di Foggia, Foggia, Italy
- ¹³² Università del Piemonte Orientale, Vercelli, Italy
- ¹³³ Università di Brescia, Brescia, Italy
- ¹³⁴ Variable Energy Cyclotron Centre, Homi Bhabha National Institute, Kolkata, India
- ¹³⁵ Warsaw University of Technology, Warsaw, Poland
- ¹³⁶ Wayne State University, Detroit, Michigan, United States
- ¹³⁷ Yale University, New Haven, Connecticut, United States
- ¹³⁸ Yildiz Technical University, Istanbul, Turkey

¹³⁹ Yonsei University, Seoul, Republic of Korea

¹⁴⁰ Affiliated with an institute covered by a cooperation agreement with CERN

¹⁴¹ Affiliated with an international laboratory covered by a cooperation agreement with CERN.